Polymer 51 (2010) 563–567

Contents lists available at ScienceDirect

Polymer

journal homepage: www.elsevier.com/locate/polymer

Evidence of sequential ordering during cold crystallization of poly (L-lactide)

Bing Na [a,*], Nana Tian [a], Ruihua Lv [a], Zhujun Li [a], Wenfei Xu [a], Qiang Fu [b,**]

[a] Department of Materials Science and Engineering, East China Institute of Technology, Fuzhou 344000, People's Republic of China
[b] Department of Polymer Science & Materials, Sichuan University, State Key Laboratory of Polymer Materials Engineering, Chengdu 610065, People's Republic of China

ARTICLE INFO

Article history:
Received 19 June 2009
Received in revised form
4 October 2009
Accepted 30 November 2009
Available online 23 December 2009

Keywords:
Sequential ordering
FTIR
Cold crystallization

ABSTRACT

The structural development during cold crystallization of poly (L-lactide) has been explored by time-dependent Fourier transform infrared spectroscopy and depolarized light scattering, respectively. It is indicated that the conformation-sensitive 956 cm^{-1} band changes first during induction period, followed by formation of 10_3 helix sequence (921 cm^{-1} band) in the disordered crystals; after that, the inner structure of new-formed disordered crystals is further perfected, giving rise to frequency shift of 871 cm^{-1} band to higher wavenumber. Moreover, the formation and subsequent perfection of disordered crystals are also evidenced by the sharp transition of integrated scattering intensity revealed by depolarized light scattering measurements. It is strongly suggested that the cold crystallization of poly (L-lactide) follows a sequential ordering or multi-step process at atomic scale. Furthermore, such a sequential ordering is independent of crystallization temperature and the thermal history (melt cooling rate) of samples prior to cold crystallization. Increasing crystallization temperature or decreasing melt cooling rate just shortens the onset time related to above-referred each step.

1. Introduction

Though extensive efforts, the molecular mechanism regarding that how random coils of a crystallizeable polymer is arranged into three-dimensional ordered crystal still remains mysterious [1–8]. In a common sense, this arrangement during polymer crystallization must involve intermolecular positional and orientational ordering as well as intramolecular conformational ordering at atomic scale, except for some specific cases where these ordering process are not necessarily coupled to each other [9]. Naturally, a question arises: do these ordering processes occur simultaneously or sequentially during polymer crystallization? In the classical crystallization theories, it is assumed that intramolecular and intermolecular ordering occurs simultaneously while a polymer chain is adsorbed on the crystal growth front to fit into the crystal lattice. In contrast, a few experiments indicate that the intramolecular conformational ordering is prior to intermolecular ordering, suggesting sequential ordering with respect to formation of ordered crystals. An example is originated from the spinodal-assisted crystallization [10,11], where the liquid–liquid separation prior to crystallization involves the coupling of density fluctuation and intramolecular conformational ordering. Another instance of sequential ordering comes from the idea of conformational regulation and pre-ordering before onset of crystallization [12,13]. It is indicated that the structural adjustment during polymer crystallization is not only cooperative but also sequential. In spite of quiescent conditions, furthermore, intramolecular conformational ordering can be decoupled with intermolecular ordering during polymer crystallization under external force [14,15], for instance shear-induced crystallization.

The evidences of sequential ordering strongly suggest that formation and growth of the ordered crystallites is not a one-step process but follows a multi-step route. Recently, Strobl has proposed that the formation of lamellae also involves a multi-step process, i.e. from the melt via mesomorphic and granular crystalline layers to lamellar crystallites [16,17]. It is suggested that the layer at crystal growth front is composed of stretched sequences with conformational defects in a liquid-like intermolecular packing. Thus, the density and anisotropy in the layer is slightly above that of the isotropic melt, away from the value in the crystals. With elapse of crystallization time, it is conjectured that the extent of ordering in this imperfect layer, including intramolecular conformational and intermolecular orientational ordering, can be further improved, giving rise to ordered crystals finally.

In this study, the structural changes during cold crystallization of PLLA have been monitored by time-dependent Fourier transform infrared spectroscopy (FTIR) and depolarized light scattering measurements, respectively. Our results indicate that the cold

* Corresponding author. Fax: +86 794 8258320.
** Corresponding author. Fax: +86 28 85405402.
E-mail addresses: bingnash@163.com, bna@ecit.edu.cn (B. Na), qiangfu@scu.edu.cn (Q. Fu).

0032-3861/$ – see front matter © 2009 Elsevier Ltd. All rights reserved.
doi:10.1016/j.polymer.2009.11.064

crystallization of PLLA follows a multi-step route at atomic scale. The intramoleuclar conformational ordering sets in first during induction period, followed by formation of 10_3 helix sequence in the disordered crystals; after that, further perfection of new-formed disordered crystals is brought out with elapse of time, giving rise to significant frequency shift of 871 cm^{-1} band as well as steep increasing of integrated scattering intensity.

2. Experimental

2.1. Material and sample preparation

A commercial poly (L-lactide) (PLLA), supplied by Brightchina Industry Corporation, China, was used in this study. It had a viscosity-average molecular weight of about 100 kg/mol, a melt flow index of 17g/10 min and a melting point of about 153 °C. Films with thickness of about 50 μm for the following FTIR, depolarized light scattering and X-ray diffraction measurements were melt-pressed in a hot stage at 190 °C. After being held for 5 min, films were quenched into ice water (referred to q-PLLA) or cooled at 10 °C/min to room temperature (designated as 10c-PLLA), respectively. Note that to avoid any possible aging effects all films were freshly prepared prior to cold crystallization measurements.

2.2. Fourier transform infrared spectroscopy (FTIR)

The as-prepared film was first inserted between two ZnSe plates and then the sandwich was fixed in the hot stage, which was placed in the sample compartment of a Thermo Nicholet FTIR spectrometer. Thereafter, the sample was heated rapidly to the desired cold crystallization temperature and held isothermally during cold crystallization. The IR spectrums at each cold crystallization temperature were collected at a resolution of 4 cm^{-1} and a total of 16 scans were added.

2.3. Depolarized light scattering (DPLS)

A polarized solid laser with a wavelength of 532 nm was applied vertically to the as-prepared film sandwiched between two glass coverslips in the hot stage that was same to that used in the FTIR measurements. The scattered light was passed through an analyzer and then onto a highly sensitive charge-coupled device (CCD) camera. Note that a small cylinder was used as a beamstop. Only depolarized Hv geometry was used for all measurements in this study, i.e. the optical axis of the analyzer was set perpendicularly to that of the polarizer. The experimental procedures of cold crystallization in the DPLS measurements were identical to those used in the FTIR measurements. The input data from the CCD camera was digitized and stored in a personal computer for further analysis. The integrated intensity over the scattering plane with q range between 0.3 and 3.2μm^{-1} was adopted to explore the formation of anisotropic objects during the early stage of cold crystallization. Note that for all data analysis the background scattering was subtracted.

2.4. X-ray diffraction (XRD)

The as-prepared films were first isothermally cold crystallized at selected temperature in the above-referred hot stage for desired period, and then quenched into ice water again. XRD measurements were conducted on an X-ray diffractometer equipped with an X-ray generator and a goniometer at room temperature. The X-rays were generated at 35 kV and 60 mA and the wavelength of the monochromated X-ray from CuK_α radiation was 0.154 nm.

3. Results and discussion

3.1. Cold crystallization of q-PLLA

Fig. 1 is the time-dependent IR spectra in the wavenumber range between 980 and 820 cm^{-1} during cold crystallization of q-PLLA at 90 °C. It is indicated that three absorption bands, located at 956,921 and 871 cm^{-1}, respectively, change significantly with elapse of time. The bands at 956 and 921 cm^{-1}, arising from the coupling of C–C backbone stretching [ν(C–COO)] and the CH_3 rocking mode [$r(CH_3)$], show inverse intensity change while their peak positions remain nearly intact. According to pioneering studies [18,19], the bands at 921 and 956 $cm^{-1}$are ascribed respectively to the crystalline α(or α') form with a 10_3 helix conformation and to the amorphous phase in the PLLA. In contrast, the increase of intensity, accompanied by peak shifting to higher wavenumber, is observed for the band at 871 cm^{-1} that is assigned to the C–C backbone stretching [υ (C–COO)]. The high frequency shifting of the band at 871 cm^{-1} is originated from the dipole–dipole interaction in the crystal lattice, an indicator of formation of ordered structure during crystallization [19,20].

To further describe the structural changes, evolution of peak intensity of above-referred bands with respect to time is deduced from the IR spectra and corresponding results are collected in Fig. 2. The intensity of each band changes little at the beginning, and then follows monotonously upward (921 and 871 cm^{-1}) or downward (956 cm^{-1}) trend, respectively, suggesting the proceeding of crystallization. Finally, at the end of crystallization each band levels off. For better understanding the intensity variation during the early stage of crystallization, an enlarged view is also given in Fig. 2. The onset time corresponding to the intensity change is determined by the interception method, as adopted by other researchers [1]. It is indicated that the intensity change of above-referred bands does not occur synchronously but follows a sequential order with time. The intensity of the band at 956 cm^{-1} changes first, followed by that at 921 cm^{-1} and then at 871 cm^{-1}, which is in accordance with other observations [18,19].

Previous studies have indicated that, in addition to the ν(C═O) stretching vibration around 1760 cm^{-1} and theν (C–O–C) skeletal vibration in the wavenumber range of 1300–1000 cm^{-1}, the vibration at 956 cm^{-1} involving the coupling of C–C backbone stretching [ν(C–COO)] and the CH_3 rocking mode [$r(CH_3)$] can be qualitatively correlated with the change of conformational state during induction period, though the conformation-sensitive bands in the FTIR spectrum of PLLA have not been clearly assigned at present [19]. Since the intensity change of 956 cm^{-1} precedes that of 921 cm^{-1} crystalline band, it can be deduced that the conformational adjustment in the entangled amorphous phase precedes

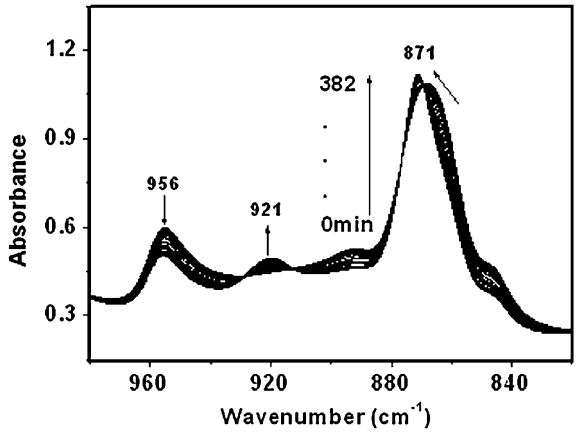

Fig. 1. Time-dependent IR spectra during cold crystallization of q-PLLA at 90 °C.

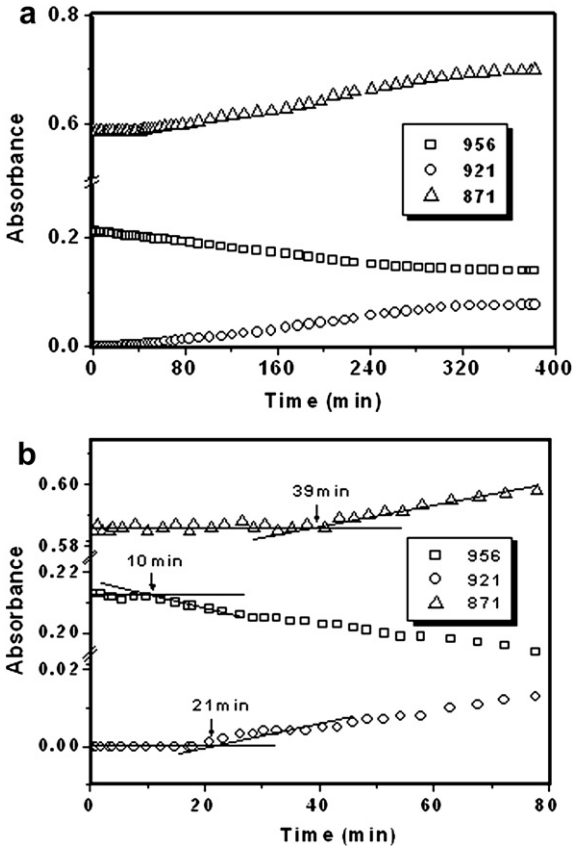

Fig. 2. Intensity change of indicated bands with time during cold crystallization of q-PLLA at 90 °C: (a) global view, and (b) enlarged view.

the formation of helix sequence in the crystals. As stated in the introduction section, conformational adjustment and pre-ordering prior to formation of crystals have been confirmed by FTIR during crystallization of poly (bisphenol A-co-decane ether) [21] and syndiotactic polystyrene [13] according to the asynchronous change between conformation- and crystalline-sensitive bands. Moreover, it has been demonstrated that during cold crystallization of PLLA at low temperature the conformational adjustment is also prior to the formation of 10_3 helix sequence arranged in the crystal lattice [19]. Considering the conformational state and conformer distribution of PLLA [22,23], furthermore, it is suggested that conformational rearrangement of PLLA from *gg* to *gt* occurs during induction period.

The conformational adjustment prior to crystallization can also be deduced from the room temperature XRD profiles of PLLA cold crystallized at 90 °C for desired period. Fig. 3 presents such results. Consistent with the structural evolution in the FTIR measurements, during induction period no crystalline diffraction peak can be observed from the XRD profiles. Until the intensity of 921 cm^{-1} crystalline band changes is the reflection of (200)/(110) crystal lattice brought out, further suggesting that the formation of 10_3 helix sequence is accompanied by the intermolecular ordering in the unit cell. The crystals formed at low temperature are imperfect, and intramolecular conformational and intermolecular orientational ordering is highly perturbed in the crystal lattice. It is manifested by periodically distorted 10_3 helical conformation and reduced specific interactions between neighboring chains [24–26]. Therefore, it is expected that further structural ordering in the crystals will proceed with elapse of time, which in turn gives rise to the emergence of other diffraction peaks, in addition to the reflection of (200)/(110) crystal lattice at later stage of cold crystallization (see Fig. 3). Note

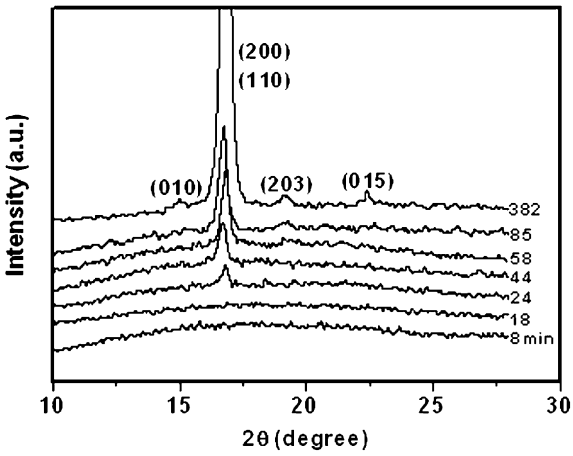

Fig. 3. Room temperature XRD profiles of q-PLLA after cold crystallization at 90 °C for desired period (indicated by the number in the legend).

that from XRD profiles it is impossible to determine the precise onset time related to such an ordering process because of significant background noise. However, the perfection of initial disordered crystals during crystallization, on the other hand, manifests itself by the lagged intensity change of 871 cm^{-1} band shown in Fig. 2. As demonstrated by Zhang et al. [18], both 871 and 921 cm^{-1} bands are belong to the 10_3 helix conformation of PLLA and their sequential order during crystallization is attributed to the different critical sequence length of helix unit (the critical sequence length is shorter for the 921 cm^{-1} band than 871 cm^{-1} band). Later, with further considering the frequency shift to higher wavenumber of 871 cm^{-1} band, Pan et al. has suggested a transition to an ordered structure during crystallization of PLLA [19]. Its rationale lies in that the frequency shift to higher wavenumber is originated from the transition dipole coupling interactions between chains contained in the unit cell of PLLA [20]. Increasing the relative orientation of interacting groups can give rise to enhanced strength of dipole–dipole interactions and thus frequency shift of 871 cm^{-1} band. Hence, it can be expected that the rotational and longitudinal defects in the initial disordered crystals have been further improved in the subsequent process of cold crystallization.

Perfection of initial disordered crystals, furthermore, is evidenced by the time-dependent depolarized integrated scattering intensity, as shown in Fig. 4. During induction period no change of integrated scattering intensity can be observed. While the crystallization sets in the orientation fluctuation from the anisotropic crystals under polarized H_v conditions gives rise to the increased integrated scattering intensity above background [1,27,28]. This argument is based on the fact that the onset time t_1 obtained from depolarized light scattering measurements is consistent with that corresponding to the intensity change of 921 cm^{-1} band. Note that the scattering patterns are isotropic during the desired period of crystallization where the crystallinity deduced from the XRD profiles is no more than 4% (the four-leaf clover pattern is observed only at late stage of cold crystallization). As mentioned above, the new-formed crystals are composed of stretched sequences with conformational defects in a liquid-like intermolecular packing, and the anisotropy (birefringence) is slightly higher than that of background. With proceeding of crystallization perfection of the initial disordered crystals can result in significant birefringence and thus the steep increasing of integrated scattering intensity can be expected. Note that at the early stage of cold crystallization it seems impossible to correlate the steep increasing of integrated scattering intensity with sharp increased volume fraction of formed crystals, i.e. crystallinity (see the intensity of 921 cm^{-1} band in Fig. 2). It is

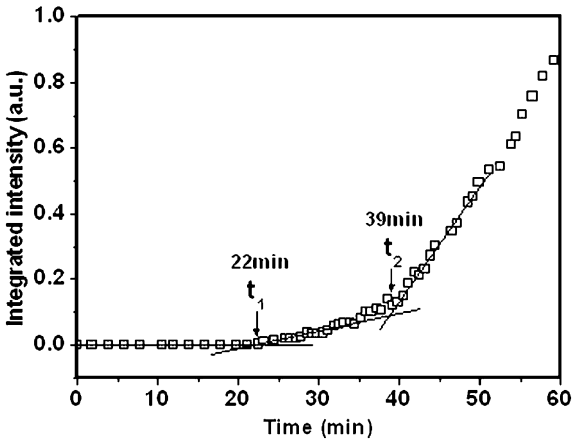

Fig. 4. Time-dependent integrated scattering intensity during cold crystallization of q-PLLA at 90 °C.

the fact in this case, and the onset time t_2 is exactly same to that related to the intensity change of 871 cm^{-1} band shown in Fig. 2. It further confirms a transition of initial disordered crystals to ordered ones at later stage of cold crystallization of PLLA.

Evidence of sequential ordering during cold crystallization of q-PLLA is also supported by the results obtained at higher temperature than 90 °C, as shown in Fig. 5. It is indicated that at each selected temperature the intramolecular conformational adjustment (956 cm^{-1} band) is always prior to formation of 10_3 helical conformation (921 cm^{-1} band), followed by a transition of initial disordered crystals to ordered ones (871 cm^{-1} band). Moreover, the onset time t_1 and t_2 related to the sharp transition of integrated scattering intensity are consistent with those corresponding to intensity change of 921 and 871 cm^{-1} band, respectively. Increasing crystallization temperature has no effect on the sequence of above-referred ordering processes and only accelerates the intramolecular conformational ordering as well as intermolecular ordering due to enhanced chain mobility at high temperature.

The above results explicitly illustrate the cold crystallization of q-PLLA follows a sequential order, as schematically shown in Fig. 6: 1) intramolecualr conformational ordering, 2) formation of 10_3 helix sequence as well as disordered crystals, 3) a transition of initial imperfect crystals to ordered ones. It means that the formation of ordered crystals during cold crystallization of q-PLLA involves

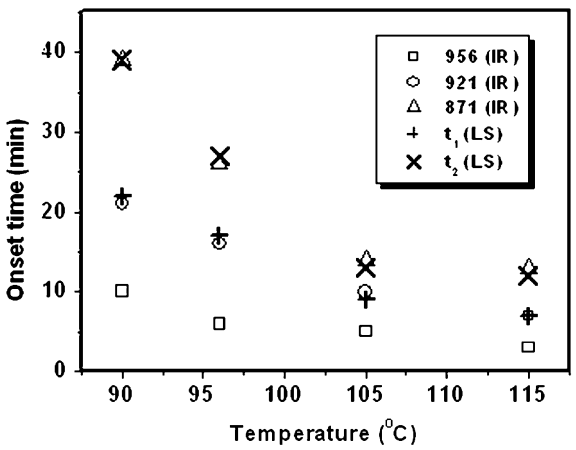

Fig. 5. Comparison of onset time of indicated bands during cold crystallization of q-PLLA at various temperatures. The onset time t_1 and t_2 related to the sharp transition of integrated scattering intensity obtained from DPLS measurements at the same conditions is also included.

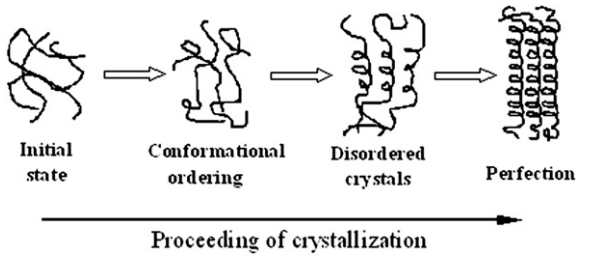

Fig. 6. Schematic diagram of sequential ordering at atomic scale during cold crystallization of PLLA.

a multi-step process. However, this multi-step process refers to the structural evolution in the unit cell at atomic scale, which is different from that proposed by Strobl [16,17]. In his crystallization model the multi-step process describes the formation of lamellar crystals at nanometer scale. May be the mesomorphic layer at the growth front of lamellae, composed of stretched sequences with conformational defects in a liquid-like intermolecular packing, is similar to the disordered crystals described in our case. And a transition of the mesomorphic layer to the granular crystals with ordered inner structure is somewhat in accordance with the perfection of disordered crystals shown in Fig. 6.

3.2. Cold crystallization of 10c-PLLA

PLLA cannot crystallize upon cooling from the melt even at 10 °C/min, giving rise to formation of amorphous glass. Even so, the

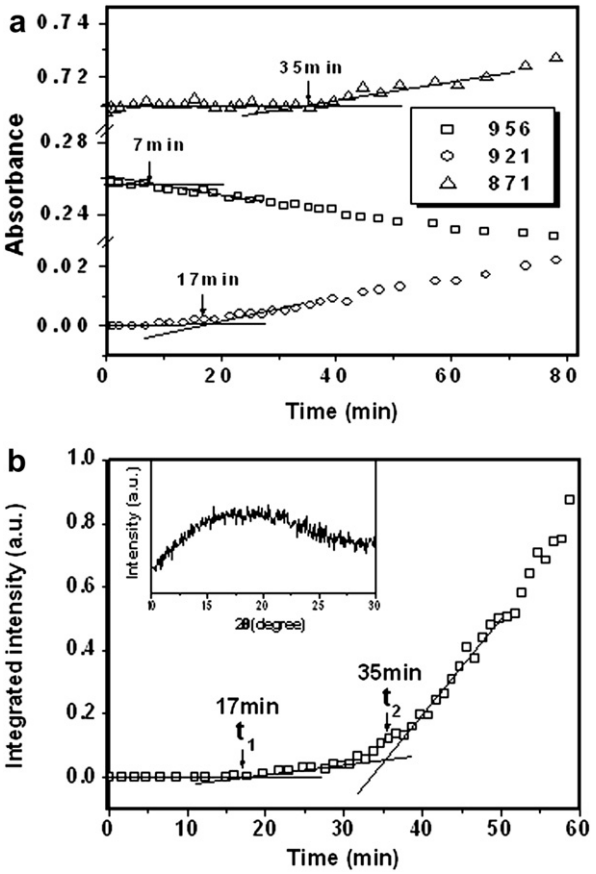

Fig. 7. Time-dependent absorbance (a) and integrated scattering intensity (b) during the early stage of cold crystallization of 10c-PLLA at 90 °C. Its XRD profile prior to cold crystallization measurements is also included in (b).

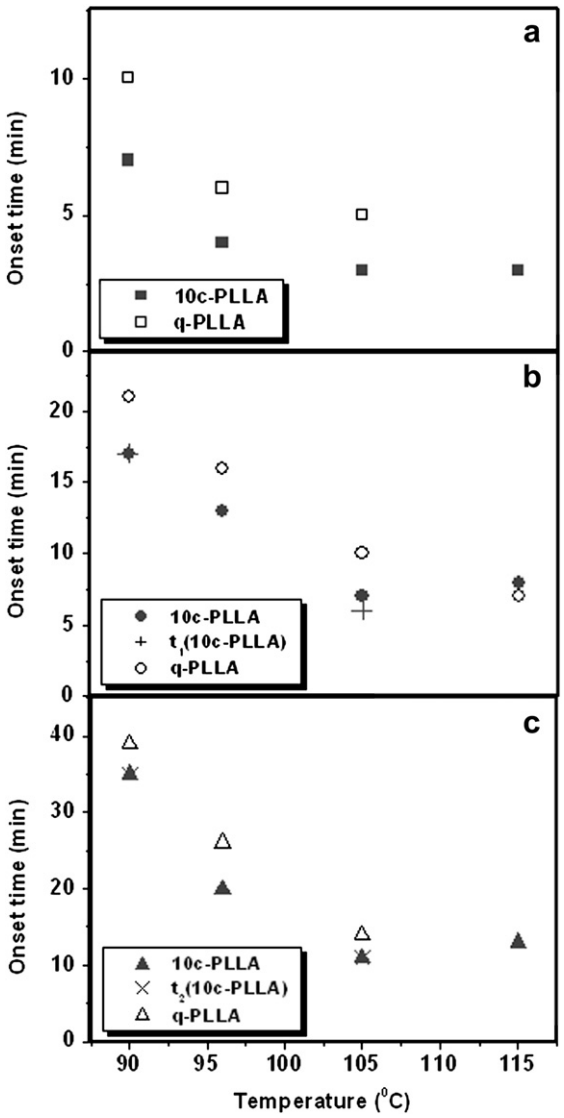

Fig. 8. Comparison of onset time of desired bands obtained from cold crystallization of PLLA with different thermal history: (a) 956, (b) 921, and (c) 871 cm^{-1}. The onset time corresponding to sharp transition of integrated scattering intensity obtained from DPLS measurements of 10c-PLLA (cooled at 10 °C/min from the melt) is also included in (b) and (c).

subsequent process of cold crystallization of such a sample can be accelerated as compared with that of quenched one [29]. It seems that the conformational adjustment and ordering occur during cooling though no crystals are formed, which further suggests the intramolecular conformational ordering can be decoupled with the intermolecular ordering related to formation of crystals. Similar arguments can also be found in a study dealing with the effect of physical aging on the crystallization kinetics and induction period of PLLA [19]. It is believed that the conformational rearrangement occurs during aging process [19,30], which in turn shortens the induction period of PLLA during subsequent cold crystallization. To further clarify this, the structural change during cold crystallization of 10c-PLLA (cooled at 10 °C/min from the melt) is monitored in this case by FTIR and DPLS measurements, respectively. The corresponding results are presented in Figs. 7 and 8. Note that the sample cooled at 10 °C/min from the melt is amorphous, indicated by absence of any diffraction peaks in the XRD profiles shown as inset in Fig. 7. Similar to that of quenched ones, as expected, the cold crystallization of 10c-PLLA also proceeds via a multi-step process, indicated by the sequential change of intensity of 956,921 and 871 cm^{-1}, respectively. Moreover, the formation and subsequent perfection of disordered crystals are also evidenced by the sharp transition of integrated scattering intensity obtained from the DPLS measurements. The difference of crystallization behavior between 10c-PLLA and q-PLLA is that decreasing melt cooling rate shortens onset time of each step, due to increased available time for conformational rearrangement during cooling process, especially while the cold crystallization temperature is no more than 105 °C (as shown in Fig. 8). At 115 °C the onset time related to each step is nearly independent of previous melt cooling rate, which may be due to the enhanced chain mobility at such a high temperature. The accelerated crystallization may overwhelm the structural pre-adjustment expected in the 10c-PLLA that cooled at 10 °C/min from the melt.

4. Conclusion

Time-dependent FTIR and DPLS measurements have explicitly confirmed that the cold crystallization of PLLA follows a sequential order at atomic scale: 1) intramolecualr conformational ordering, 2) formation of 10_3 helix sequence as well as disordered crystals, 3) a transition of initial imperfect crystals to ordered ones. Moreover, increasing crystallization temperature or decreasing melt cooling rate has no influence on the sequence of above-referred ordering processes, and only shortens the onset time of each step in such a multi-step process.

Acknowledgement

This work is supported by the National Natural Science Foundation of China (No. 20704006 and 50973017) and the Project of Jiangxi Provincial Department of Education (No. GJJ08295).

References

[1] Wang ZG, Hsiao B, Sirota E, Agarwal P, Srinivas S. Macromolecules 2000; 33:978–89.
[2] Hikosaka M, Yamazaki S, Wataoka I, Ch.Das N, Okada K, Toda A, et al. Macromol Sci Phys 2003;42:847–65.
[3] Lotz B. Eur Phys J 2000;E3:185–94.
[4] Lauritzen J, Hoffman J. J Appl Phys 1973;44:4340–52.
[5] Iijima M, Strobl G. Macromolecules 2000;33:5204–14.
[6] Cheng SZD, Janimak J, Zhang A, Cheng H. Macromolecules 1990;23:298–303.
[7] Cheng SZD, Li CY, Zhu L. Eur Phys J 2000;E3:195–7.
[8] Hu W, Cai T. Macromolecules 2008;41:2049–61.
[9] Wunderlich B, Grebowicz J. Adv Polym Sci 1984;60:1–59.
[10] Kaji K, Nishida K, Kanaya T, Matsuba G, Konishi T, Imai M. Adv Polym Sci 2005;191:187–240.
[11] Olmsted PD, Poon WCK, McLeish CB, Terrill NJ, Ryan AJ. Phys Rev Lett 1998;81:373–6.
[12] Matsuba G, Kaji K, Nishida K, Kanaya T, Imai M. Macromolecules 1999;32: 8932–7.
[13] Zhang J, Duan Y, Sato H, Shen D, Yan S, Noda I, et al. Phys Chem B 2005;109: 5586–91.
[14] Abou-Kandil A, Windle A. Polymer 2007;48:5069–79.
[15] An H, Zhao B, Ma Z, Shao C, Wang X, Fang Y, et al. Macromolecules 2007;40:4740–3.
[16] Strobl G. Eur Phys J 2000;E3:165–83.
[17] Heck B, Hugel T, Iijima M, Strobl G. Polymer 2000;41:8839–48.
[18] Zhang J, Tsuji H, Noda I, Ozaki Y. J Phys Chem B 2004;108:11514–20.
[19] Pan P, Liang Z, Zhu B, Dong T, Inoue Y. Macromolecules 2008;41:8011–9.
[20] Meaurio E, Lpez-Rodrguez N, Sarasua JR. Macromolecules 2006;39:9291–301.
[21] Jiang Y, Gu Q, Li L, Shen DY, Jin XG, Chan CM. Polymer 2004;44:3509–13.
[22] Meaurio W, Zuza E, López-Rodríguez N, Sarasua JR. J Phys Chem B 2006;110:5790–800.
[23] Zhang J, Tashiro K, Tsuji H, Domb AJ. Macromolecules 2008;41:1352–7.
[24] Kawai T, Rahman N, Matsuba G, Nishida K, Kanaya T, Nakano M, et al. Macromolecules 2007;40:9463–9.
[25] Cho T, Strobl G. Polymer 2006;47:1036–43.
[26] Zhang J, Tashiro K, Domb A, Tsuji H. Macromol Symp 2006;242:274–8.
[27] Hoffmann A, Strobl G. Polymer 2003;44:5803–9.
[28] Baert J, Puyvelde P. Macromol Mater Eng 2008;293:255–73.
[29] Snchez M, Mathot V, Poel G, Ribelles J. Macromolecules 2007;40:7989–97.
[30] Pan P, Zhu B, Inoue Y. Macromolecules 2007;40:9664–71.